South Asian J. Zool., vol. 44(2), pp 123-137, 2026 DOI: https://dx.doi.org/10.17582/sajz/2026/44.2.123.137



Molecular Docking and Pharmacokinetic Profiling of *Capparis spinosa* Fruit Phytochemicals Targeting HMG-CoA Reductase and NPC1L1 against Hypercholesterolemia

Qurban Ali[1], Erum Zafar[1], Asma Arshad[1], Aisha Jamshed[2], Junaid Ahmad[1] and Muhammad Khan[1]*

[1]*Cancer Research Lab, Institute of Zoology, University of the Punjab, Quaid-e-Azam Campus, Lahore 54590, Pakistan*
[2]*Department of Biological Sciences, Virtual University of Pakistan, Pakistan*

Qurban Ali and Erum Zafar contributed equally in this manuscript.

Article Information
Received 07 April 2026
Revised 25 October 2026
Accepted 11 November 2026
Available online 25 November 2026

Authors' Contribution
QA: Investigation, methodology, formal analysis, data curation, software, visualization. EZ: Investigation, methodology, formal analysis, data curation. QA, EZ: Writing-original draft. AA: Methodology, validation, visualization. AJ: Validation, investigation. JA: Conceptualization, supervision, resources. MK: Conceptualization, supervision, project administration, resources. AA, MK, JA: Writing-review and editing.

Key words
***Capparis decidua*, Niemann–Pick C1-like 1, HMG-CoA reductase, Molecular docking, Pharmacokinetics, Hypercholesterolemia, Medicinal plants**

ABSTRACT

Hypercholesterolemia is a major risk factor for atherosclerotic cardiovascular diseases, and long-term use of lipid-lowering drugs may cause adverse effects, emphasizing the need for safer alternatives. This study evaluated the bioactive constituents of *Capparis spinosa* (CPS) fruit against two key regulators of cholesterol metabolism, HMG-CoA reductase (PDB: 1DQ8) and Niemann–Pick C1-like 1 (NPC1L1), using molecular docking and pharmacokinetic screening in open (3GKI) and closed (3QNT) states. Twenty-five secondary metabolites were compared with standard agents Atorvastatin and Ezetimibe. Several phytochemicals exhibited lowest binding energies than the standard drugs. Quercetin displayed the most favorable binding energies (–9.4 kcal/mol with NPC1L1-open, –7.8 with NPC1L1-closed, –8.6 with HMG-CoA reductase). Ginkgetin, isoginkgetin, daucosterol, β-carotene, and sakuranetin also showed favorable interactions, whereas small polar molecules such as tetrahydropyran-2-one and uracil showed binding energies in the range of –4.7 to –5.3kcal/mol. SwissADME analysis indicated good oral bioavailability and acceptable drug-likeness for all ligands. These findings suggest that flavonoids, phytosterols, and carotenoids from CPS have the potential to inhibit both cholesterol absorption and biosynthesis. Further *in vitro* and *in vivo* studies are required to validate these computational results and assess the safety, efficacy, and bioavailability of these formulations for potential development as natural lipid-lowering agents.

INTRODUCTION

High level of total cholesterol or low-density lipoprotein cholesterol in human blood leads to hypercholesterolemia, which indicates an alarming point for atherosclerotic cardiovascular diseases (CVDs) with coronary artery disease, peripheral vascular disease, and stroke (Goldstein, 1974). The mutated LDL receptor (LDLR), PCSK9, and apolipoprotein B (APOB), are distinguished into primary and secondary genetic disorders (Khera and Hegele, 2020; Wilemon *et al*., 2020). About 39% of the total global adults are affected by hypercholesterolemia, including the increase in optimum range of LDL-C, contributing to global cardiovascular diseases and deaths (Timmis *et al*., 2022). The death rate decreased until 2010, after which it accelerated and exceeded in 2018. The number of affected persons was adults, with an older age ratio of 58.4% in Korea (Lee *et al*., 2021). Predicted from the data from 1999 to 2020, level of LDL-C in the United States is increasing (Sayed *et al*., 2023). Approximately, 20 to 25% of the total adult population in Pakistan is affected by hypercholesterolemia, besides genetic and sporadic forms (Zeeshan *et al*., 2023).

Hypercholesterolemia can occur in many forms. Familial hypercholesterolemia (FH) occurs due to genetic mutations, and an early age elevation of LDL-C occurs due to a monogenic disorder, which leads to heart disease (Nordestgaard *et al*., 2013). The medicines that control LDL-C and CVD risk, like statins, ezetimibe, bile acid

* Corresponding author: mkhan.zool@pu.edu.pk
1013-3461/2025/0001 $ 0.00/0

Copyright 2025 by the authors.
This article is an open access article distributed under the terms and conditions of the Creative Commons Attribution (CC BY) license (https://creativecommons.org/licenses/by/4.0/).

sequestrants, newer agents like bempedoic acid, and PCSK9, are available in the market (Bove *et al*., 2019). With that, the marketed medicines have severe side effects on human health like liver diseases, myopathy, and glucose intolerance, due to cost and availability in low-resource settings (von Känel-Cordoba *et al*., 2024).

Niemann-Pick C1-Like 1 (NPC1L1) is a polytopic transmembrane protein primarily expressed on the apical membrane of small intestinal enterocytes and, to a lesser extent, in human and primate hepatocytes. It functions as the principal sterol transporter responsible for the uptake of dietary and biliary cholesterol, as well as plant sterols, from the intestinal lumen into enterocytes through a clathrin/AP2-mediated vesicular endocytosis process. This mechanism makes NPC1L1 essential for intestinal cholesterol absorption, helping to counterbalance hepatobiliary cholesterol excretion and playing a central role in whole-body cholesterol homeostasis. It is the direct molecular target of the cholesterol absorption inhibitor ezetimibe, which blocks sterol-induced internalization of NPC1L1 (Ge *et al*., 2008).

HMG-CoA reductase (3-hydroxy-3-methylglutaryl-coenzyme A reductase) is the rate-limiting enzyme in the mevalonate pathway of de novo cholesterol biosynthesis. Located in the endoplasmic reticulum, it catalyzes the irreversible NADPH-dependent conversion of HMG-CoA to mevalonic acid, thereby controlling the overall flux toward cholesterol and other essential isoprenoids. The enzyme is tightly regulated at transcriptional, post-transcriptional, and post-translational levels and serves as the primary pharmacological target of statin drugs, which competitively inhibit it to suppress endogenous cholesterol production and lower circulating LDL-cholesterol levels (Xue *et al*., 2025).

Medicinal plants offer a viable avenue for developing novel hypercholesterolemic medicines due to their multitarget action, bioactive secondary metabolites, decreased toxicity, and cultural acceptability (Sarkar *et al*., 2025). Different ethnobotanical and pharmacological studies have identified plant-derived compounds capable of modulating lipid metabolism, with flavonoids, alkaloids, and saponins (Coghlan *et al*., 2015; Rathee *et al*., 2010). The use of traditional plants for ailments other than their traditional uses is an advanced approach, and their comparison with evidence-based drugs ensures their utility, safety, and scientific verification (Axiotis *et al*., 2018; Fung and Linn, 2015).

Several traditionally used medicinal plants have demonstrated potential in managing hypercholesterolemia through lipid-lowering effects, often attributed to their rich content of bioactive compounds such as flavonoids, sterols, saponins, and dietary fiber. *Capparis spinosa* L. (CPS), a perennial shrub native to the Mediterranean region and distributed across parts of Western Asia, has a long history of traditional medicinal and dietary use. Various plant parts, including the flower buds, fruits, leaves, roots, and seeds, contain diverse phytochemicals, particularly flavonoids, phenolic compounds, alkaloids, glucosinolates, and sterols. These constituents have been investigated for their antioxidant, anti-inflammatory, and other biological activities. Although experimental studies have explored the potential metabolic benefits of CPS evidence supporting consistent improvements in cardiovascular risk markers and lipid profiles remains limited and varies according to the plant part, extraction method, and preparation used (Annaz *et al*., 2022). Therefore, the potential contribution of CPS to cholesterol regulation warrants further investigation, including controlled studies to establish its effects on cholesterol absorption, lipid metabolism, and relevant biochemical markers.

In this study, we have explored the phytoactive compounds of CPS fruit against HMG-CoA reductase and Niemann-Pick C1-like protein 1 (NPC1L1). These proteins are directly involved in regulating cholesterol levels in both the cell and the blood of the human body.

MATERIALS AND METHODS

Protein preparation

Two target proteins that are HMG-CoA reductase (PDB ID: 1DQ8) and NPC1L1 with two conformational phases, i.e., open conformation (PDB ID: 3GKI) and closed conformation (PDB ID: 3QNT) were selected for molecular docking studies. Protein structures were retrieved from the Protein Data Bank (PDB). Before docking, all native ligands and protein were prepared using our standard protocol as discussed in our previous study (Hassan *et al*., 2024; Jamshed *et al*., 2025).

Ligand preparation

We selecte a total of 25 compounds from the published literature (Annaz *et al*., 2022). All the ligands were retrieved from PubChem in SDF format and converted to PDB format using the standard protocol as discussed in our previous studies (Hassan *et al*., 2024; Jamshed *et al*., 2025).

Molecular docking

Molecular docking was performed using AutoDock 4.2. For each protein-ligand complex, a grid box was generated with dimensions set at 40 × 40 × 40 along the x, y, and z axes. For HMG-CoA reductase, x, y and z was generated at 26.119, 16.963 and -15.762, respectively. For 3GKI x, y, and z coordinates were generated at -32.531,

-32.656 and 3.895 while 3QNT was generated at -16.044, -24.570, and 11.676, respectively at the active site of the protein. Docking parameters were set to generate nine conformational poses for each ligand. The best binding pose was selected based on the lowest binding energy and was then analyzed further for its binding interactions.

Pharmacokinetics profiling

The pharmacokinetic properties and drug-likeness of the selected ligands were evaluated using the SwissADME online tool. The Lipinski's rule of five was evaluated for each ligand.

RESULTS

In this study, we identified 25 phytochemical compounds of CPS fruit against two targeted proteins involved in cholesterol metabolism that are HMG-CoA reductase and NPC1L1 (open and closed state). The binding energies were compared with two standard drugs, Atorvastatin and Ezetimib. The atorvastatin showed binding energies for 3GKI and 3QNT are -6.4 kcal/mol and -6.1 kcal/mol, respectively, while HMG-CoA reductase (1DQ8) showed -5.4kcal/mol. However, ezetimib showed -6.3 kcal/mol with 3GKI and -6.0 kcal/mol with 3QNT and -7.3kcal/mol with HMG-CoA reductase.

Molecular docking analysis

A total of 25 phytoactive compounds from CPS fruit were subjected to molecular docking against NPC1L1 (3GKI and 3QNT) and HMG-CoA reductase (1DQ8). The binding energies of all docked complexes are summarized in Table I.

Table I. All the compounds along with CID, binding energies and inhibition constant.

S. No.	Compound	Pubchem (ID)	Inhibition Constant (uM)	Binding energies (Kcal/mol)				
				HMG-CoA reductase (1DQ8)	NPC1L1 (3GKI)	NPC1L1 (3QNT)	Arovas-tatatin	Eze-timibe
1	1-H Indole-3-acetonitrile	13805944	46.7	-5.9	-7.0	-6.7	-5.4	-9.1
2	5- (Hydroxymethyl)-D	448088	5.30	-7.2	-5.4	-6.0	-5.4	-9.1
3	Beta-Carotene	5280489	91.4	-5.5	-10	-6.6	-5.4	-9.1
4	Biflavonoid	161259	23.7	-6.3	-7.8	-7.2	-5.4	-9.1
5	Cadabicine	6442583	149	-5.3	-8.6	-8.1	-5.4	-9.1
6	Corchoionoside C	10317980	1.25	-7.5	-7.8	-6.5	-5.4	-9.1
7	Daucosterol	5742590	0.042	-8.7	-7.9	-6.0	-5.4	-9.1
8	Flavonoid	11349	1.58	-7.4	-9.3	-6.2	-5.4	-9.1
9	Ginkgetin	5271805	0.034	-8.8	-9.3	-7.6	-5.4	-9.1
10	Glucosinolates	9576738	1.96	-7.3	-6.6	-6.9	-5.4	-9.1
11	Hydrocinnamic acids	107	46.7	-5.9	-6.4	-6.0	-5.4	-9.1
12	Isodulcite	5460029	37.6	-6.0	-4.9	-5.5	-5.4	-9.1
13	Isoginkgetin	5318569	0.042	-8.7	-8.9	-8.2	-5.4	-9.1
14	Methylstachydrine	117064719	278	-5.0	-5.7	-5.7	-5.4	-9.1
15	Phthalic acid	1017	35.3	-6.2	-6.3	-6.7	-5.4	-9.1
16	P-hydrobenzoic acid	520781	108	-5.6	-6.7	-5.5	-5.4	-9.1
17	P-hydroxyl benzoic acid	21426294	92.7	-5.7	-6.9	-6.3	-5.4	-9.1
18	Quercitin	5280343	0.054	-8.6	-9.4	-7.8	-5.4	-9.1
19	Sakuranetin	73571	0.96	-7.7	-9.0	-6.7	-5.4	-9.1
20	Stachydrine	115244	442	-4.7	-5.3	-5.5	-5.4	-9.1
21	Vitamin C	54670067	23.7	-6.3	-6.1	-6.0	-5.4	-9.1
22	2-Carboxy-1-dimethylpyrrolidine	4479243	278	-5.0	-5.5	-5.6	-5.4	-9.1
23	Cappaprenol-12	6440455	325	-4.9	-5.6	-3.9	-5.4	-9.1
24	Tetrahydropyran-2-one	10953	442	-4.7	-4.7	-4.7	-5.4	-9.1
25	Uracil	1174	238	-5.1	-4.9	-5.3	-5.4	-9.1

Table II. Molecular docking interactions of selected compounds with 1DQ8 and NPC1L1 (3GKI/3QNT) showing amino acid residues, interaction types, distances, and binding energies.

Ligand name (CID)	Protein PDB ID	Interaction amino acid residues (Distance: Å)	Binding energy (Kcal/mol)
Corchoionoside C (10317980)	1DQ8	Hydrogen bond: ILE638, ILE699, SER637 Hydrophobic (alkyl, π-alkyl): HIS635, LYS633, ALA585	-7.6
	NPC1L1 (3GKI/3QNT)	Conventional Hydrogen bond: ILE218, ASN204, VAL191, GLN79, ASN41, ASN198 Carbon-Hydrogen bond: GLY190, ASP208, MET193 Hydrophobic: TYR192, LEU111, ILE205, PRO202, LEU83, PHE203	-7.8/-6.5
Daucosterol (5742590)	1DQ8	Conventional Hydrogen bond: VAL583 Hydrophobic (alkyl, π-alkyl): LYS633, HIS635	-8.7
	NPC1L1 (3GKI/3QNT)	Conventional Hydrogen bond: LYS107, ASP118, SER117, SER45, GLU43 Hydrophobic (alkyl, π-alkyl): VAL97, ILE77, LYS76, PRO52, VAL77, CYS42, TYR28, TYR44	-7.9/-6.0
Ginkgetin (5271805)	1DQ8	Conventional Hydrogen bond: LEU634, SER705 Carbon-Hydrogen bond: GLN632 Hydrophobic (alkyl, π-alkyl): VAL583, LYS633, LYS606 Van der Waals: HIS635, ALA585	-8.8
	NPC1L1 (3GKI/3QNT)	Conventional Hydrogen bond: ASN222, SER72, GLN88 Hydrophobic (alkyl, π-alkyl): PRO131, PRO115	-9.3/-7.6
Glucosinolate (9576738)	1DQ8	Conventional Hydrogen bond: THR636, ILE699, HIS635, GLN648 Carbon-Hydrogen bond: GLU610 Hydrophobic: ALA585, LYS633	-7.1
	NPC1L1 (3GKI/3QNT)	Conventional Hydrogen bond: ASN204, ASP208, ILE218, THR Hydrophobic (alkyl, π-alkyl): LEU91, LEU87, LEU62, LEU105, LYS84, ARG201 Additional Hydrogen bond: TYR192	-6.6/-6.9
Isoginkgetin (5318569)	1DQ8	Conventional Hydrogen bond: GLN632, SER637, GLN648 Hydrogen bond: GLU610, THR636 Hydrophobic (alkyl, π-alkyl): LYS633, PRO798, LYS606, ALA585	-8.7
	NPC1L1 (3GKI/3QNT)	Conventional Hydrogen bond: GLU238, GLN88, GLY65 Carbon-Hydrogen bond: LEU81, ASN132 Hydrophobic (alkyl, π-alkyl, π-sigma): PRO131, CYS63, CYS109, THR83, HIS126	-8.9/-8.2
Quercetin (5280343)	1DQ8	Conventional Hydrogen bond: GLU200, TRP698, SER637, LYS606 Carbon-Hydrogen bond: HIS635 Hydrophobic (π-anion, π-alkyl): GLU610, PRO798, ALA585	-8.6
	NPC1L1 (3GKI/3QNT)	Conventional Hydrogen bond: SER56, GLU38, SER102, GLN79, ARG39, MET193 π-Donor Hydrogen bond: ASN41 Hydrophobic (π-T shaped, π-alkyl): PHE108, GLN200, PRO215, LEU103, ALA201, PRO202	-9.4 / -7.8
Sakuranetin (73571)	1DQ8	Conventional Hydrogen bond: SER637, ILE638 Carbon-Hydrogen bond: HIS635 Hydrophobic (π-cation, π-stacked, π-alkyl): LYS606, PRO798, GLU610	-8.6
	NPC1L1 (3GKI/3QNT)	Conventional Hydrogen bond: SER53, ASN86, THR112 Carbon-Hydrogen bond: SER102, LEU213 Hydrophobic (alkyl, π-alkyl): ARG39, PRO202, PHE203, PHE108, LEU52, ILE105	-9.0/-6.7

For NPC1L1 in both 3GKI and 3QNT showed strong binding affinities in the range -3.9 kcal/mol to -10 kcal/mol. 3GKI showed the lowest binding energies were observed for β-carotene (−10.0 kcal/mol), quercetin (−9.4 kcal/mol), sakuranetin (−9.0 kcal/mol), ginkgetin (−9.3 kcal/mol), and flavonoids (−9.3 kcal/mol). However, 3QNT exhibit lowest binding energies with quercetin (−7.8 kcal/mol), isoginkgetin (−8.2 kcal/mol), and cadabicine (−8.1 kcal/mol). Docking analysis against 1DQ8 revealed that ginkgetin (−8.8 kcal/mol), daucosterol (−8.7 kcal/mol), isoginkgetin (−8.7 kcal/mol), quercetin (−8.6 kcal/mol), corchoionoside C (−7.6 kcal/mol), and Glucosinolate (−7.1 kcal/mol) showed the strongest binding affinities, comparable to the reference drug atorvastatin (−5.4 kcal/mol) (Table II).

Based on docking scores, seven compounds that are corchoionoside C, daucosterol, ginkgetin, Glucosinolate, isoginkgetin, quercetin, and sakuranetin were selected for detailed interaction analysis. Corchoionoside C in complex with 1DQ8 showed conventional hydrogen bondingwith

ILE638. ILE699, SER637 amino acid residues while hydrophobic interactions (alkyl and π-alkyl) were shown with HIS635, LYS633, and ALA585 amino acid residues. However, in complex with NPC1L1, it showed conventional hydrogen bonding with ILE218, ASN204, VAL191, GLN79, ASN41, ASN198 while carbon-hydrogen bonding was shown with GLY190, ASP208, MET193 amino acid residues. Moreover, hydrophobic interactions were shown with TYR192, LEU111, ILE205, PRO202. LEU83 and PHE203 amino acid residues (Fig. 1).

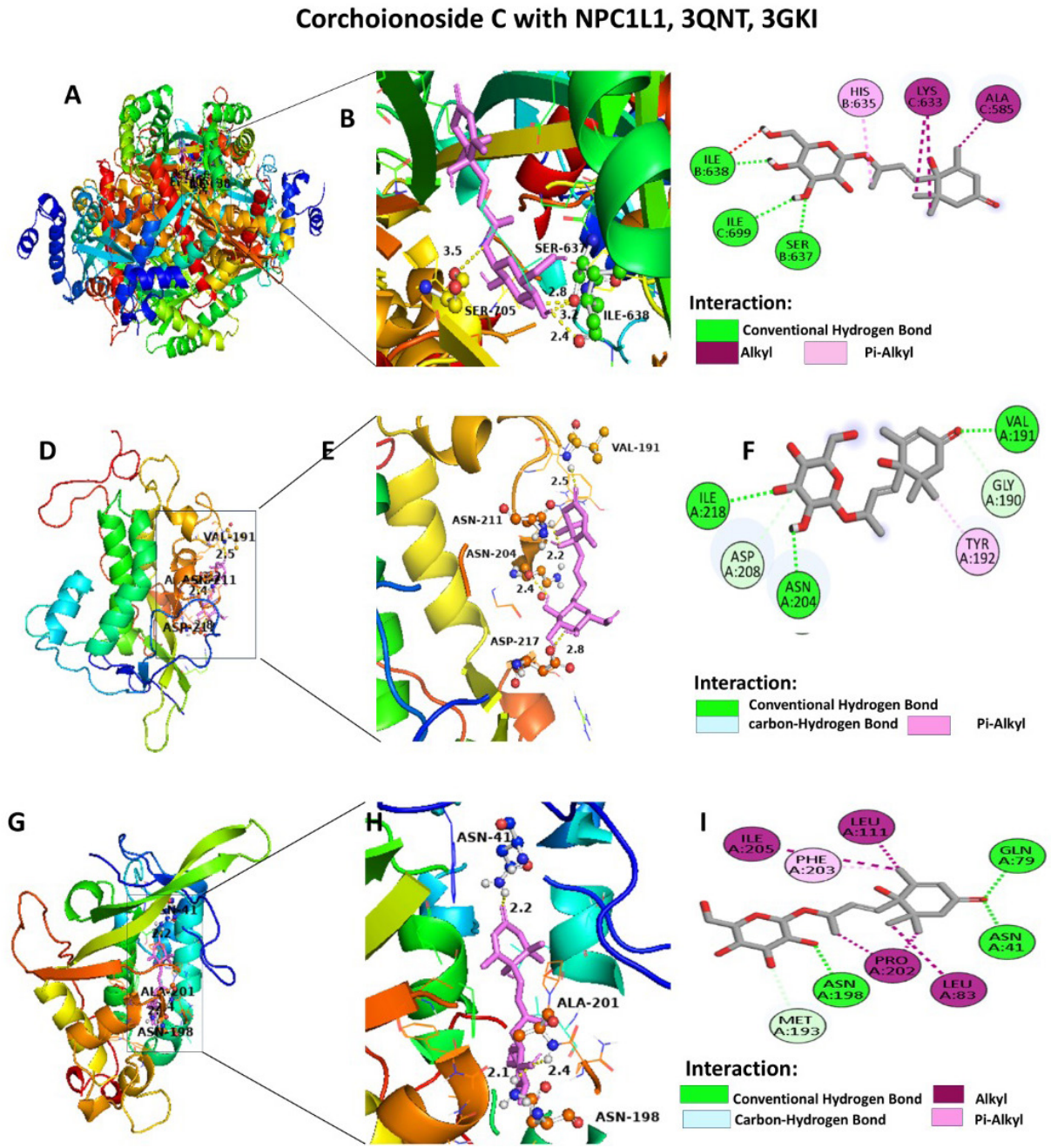


Fig. 1. Interactions between ligand corchoionoside C with two proteins named 1DQ8 and NPC1L1 (3QNT, and 3GKI), respectively. A, B and C show the NPC1L1- Corchoionoside C complex's interaction, while D, E and F show the 3QNT- Corchoionoside C complex's interaction, and G, H and I show the 3GKI- Corchoionoside C complex's interaction through PyMOL and Discovery Studio Visualizer.

Daucosterol in complex with 1DQ8 showed conventional hydrogen bonding with VAL583, amino acid residues, while hydrophobic interactions (alkyl and π-alkyl) were shown with LYS633, and HIS635 amino acid residues. However, in complex with NPC1L1, it showed conventional hydrogen bonding with LYS107, ASP118, SER117, SER45, and GLU43. Moreover, hydrophobic interactions (alkyl and π-alkyl) VAL97, ILE77, LYS76, PRO52, VAL77, CYS42, TYR28, and TYR44 with animo acid residues (Fig. 2).

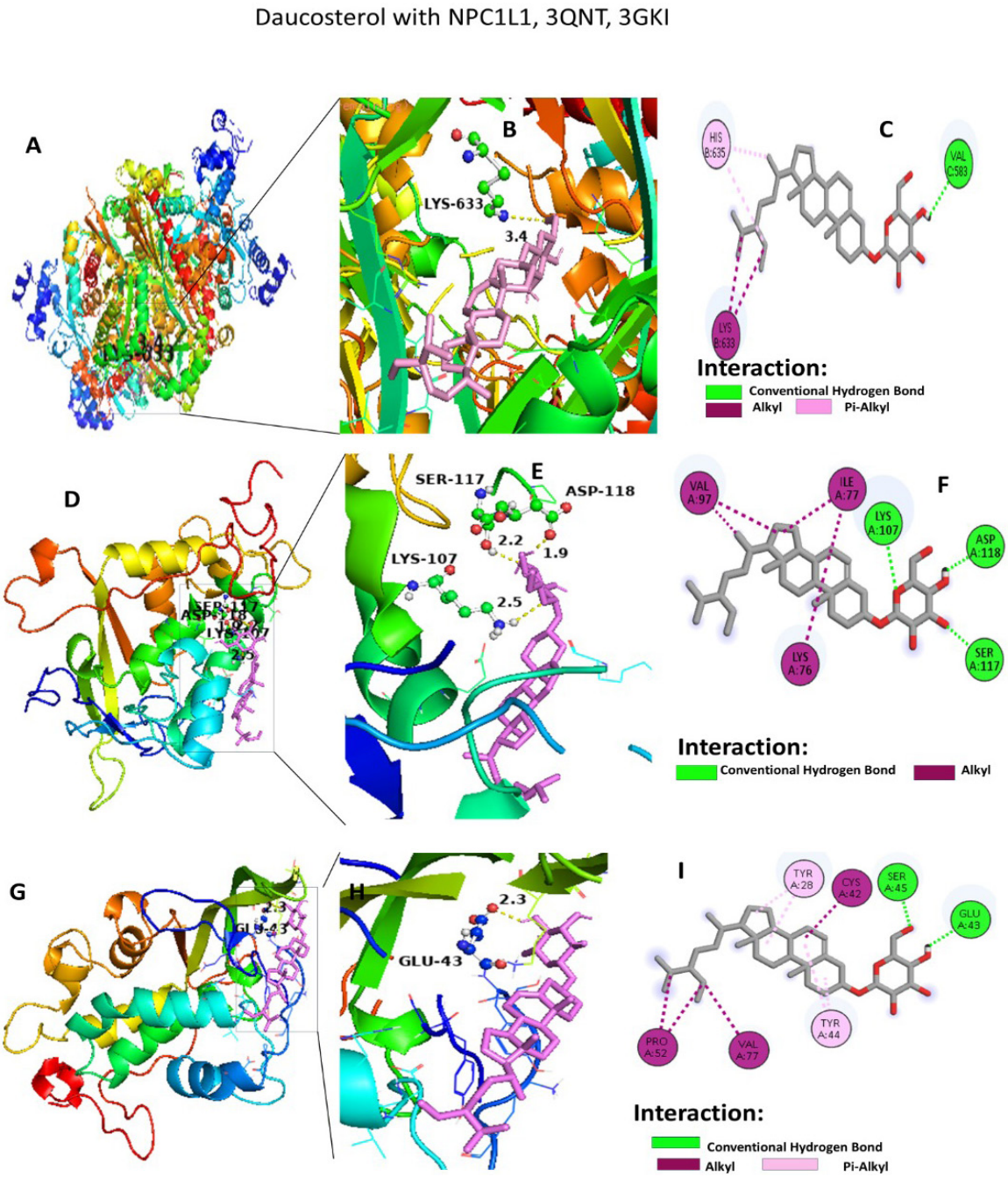


Fig. 2. Interactions between ligand daucosterol with two proteins named 1DQ8 and NPC1L1 (3QNT, and 3GKI), respectively. A, B and C show the NPC1L1- Daucosterol complex's interaction, while D, E and F show the 3QNT- Daucosterol complex's interaction, and G, H and I show the 3GKI- Daucosterol complex's interaction through PyMOL and Discovery Studio Visualizer.

Ginkgetin in complex with 1DQ8 showed conventional hydrogen bonding with LEU634, and SER705 amino acid residues, while hydrophobic interactions (alkyl and π-alkyl) were shown with VAL583, LYS633, LYS606 amino acid residues. While carbon hydrogen bonding was shown with GLN632 amino acid residues. While vander waals interactions were shown with HIS635, ALA585 amino acid residues. However, in complex with NPC1L1, it showed conventional hydrogen bonding with ASN222, SER72, and GLN88 amino acid residues. Moreover, hydrophobic interactions (alkyl and π-alkyl) were shown with PRO131, and PRO115 amino acid residues (Fig. 3).

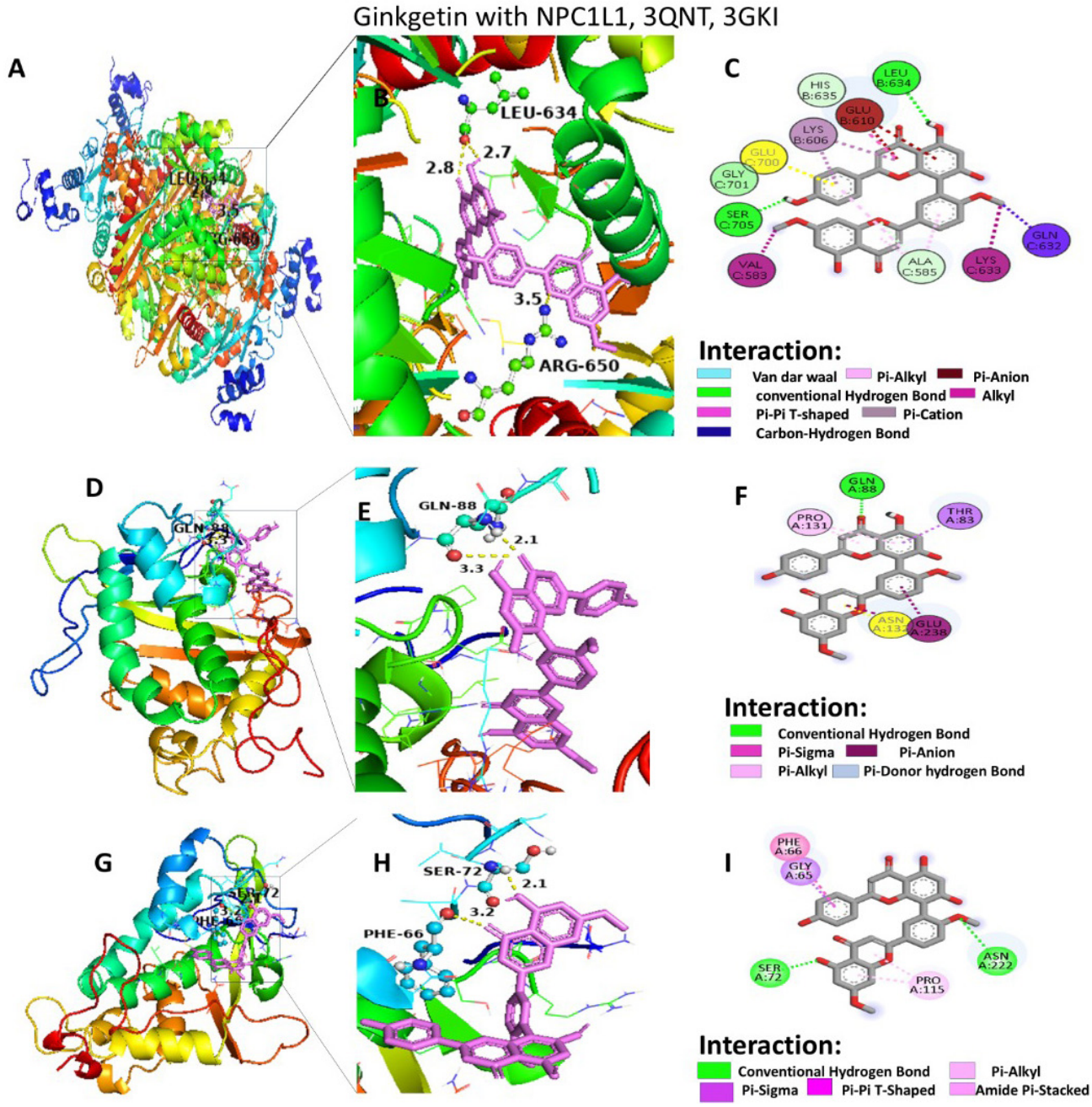


Fig. 3. Interactions between ligand ginkgetin with two proteins named 1DQ8 and NPC1L1 (3QNT, and 3GKI), respectively. A, B and C show the NPC1L1- ginkgetin complex's interaction, while D, E and F show the 3QNT- Ginkgetin complex's interaction, and G, H and I show the 3GKI- Ginkgetin complex's interaction through PyMOL and Discovery Studio Visualizer.

Glucosinolate in complex with 1DQ8 showed conventional hydrogen bonding with THR636, ILE699, HIS635, and GLN648 amino acid residues, while carbon hydrogen bonding interactions were shown with GLU610 amino acid residues. While hydrophobic interactions were shown with ALA585, and LYS633 amino acid residues. However, in complex with NPC1L1, it showed conventional hydrogen bonding with ASN204, ASP208, ILE218, and THR amino acid residues. Moreover, hydrophobic interactions (alkyl and π-alkyl) were shown with LEU91, LEU87, LEU62, LEU105, LYS84 and ARG201 amino acid residues. Moreover, hydrogen bonding interactions shown with TYR192 amino acid residue (Fig. 4).

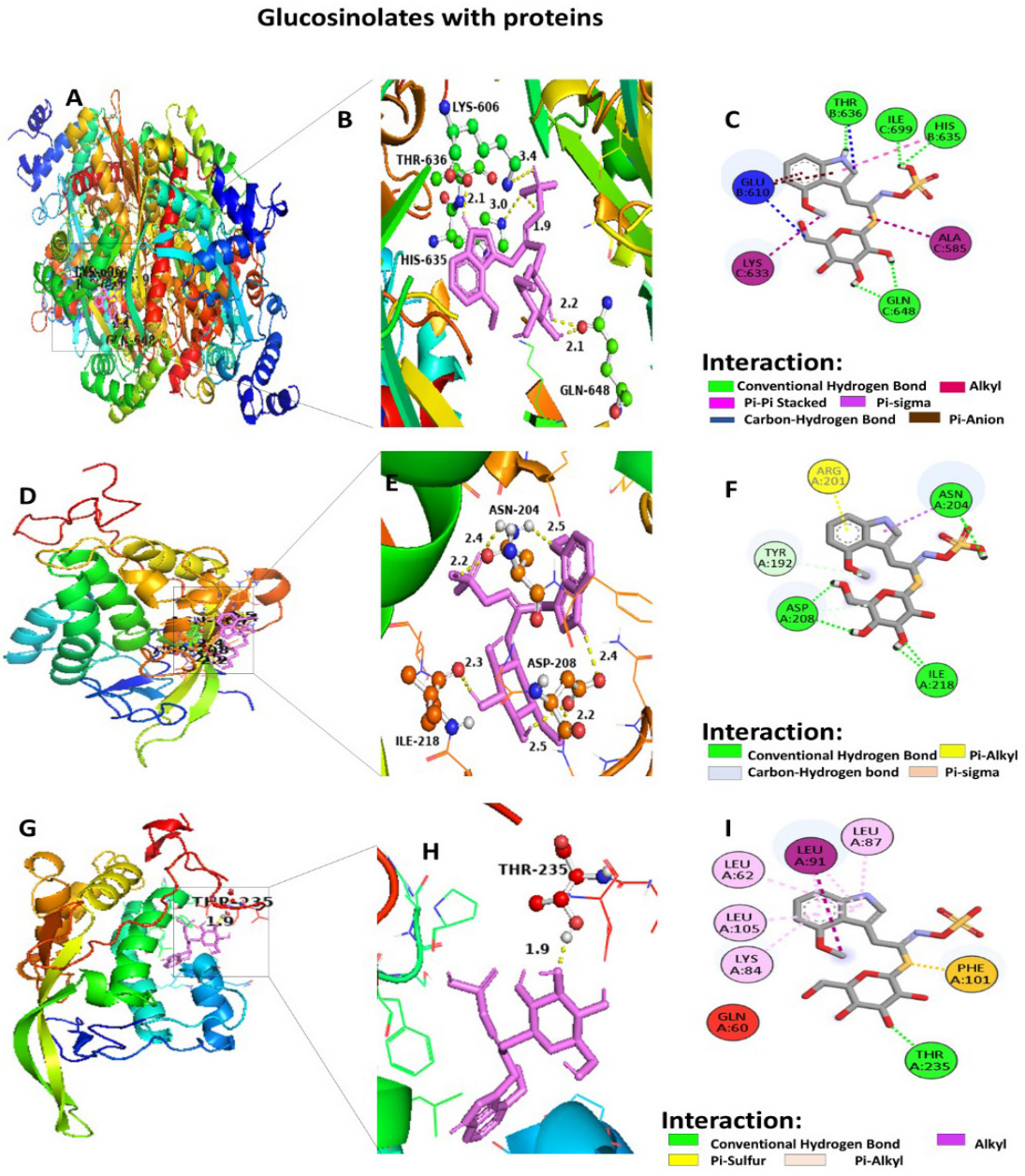


Fig. 4. Interactions between ligand glucosinolate with two proteins named 1DQ8 and NPC1L1 (3QNT, and 3GKI), respectively. A, B and C show the NPC1L1- Glucosinolate complex's interaction, while D, E and F show the 3QNT-Glucosinolate complex's interaction, and G, H and I show the 3GKI-Glucosinolate complex's interaction through PyMOL and Discovery Studio Visualizer.

Isoginkgetin in complex with 1DQ8 showed conventional hydrogen bonding with GLN632, SER637, and GLN648 amino acid residues, while hydrophobic interactions (alkyl and π-alkyl) were shown with LYS633, PRO798, LYS606, ALA585, and LYS633 amino acid residues. While hydrogen bonding interaction were shown with GLU610, and THR636 amino acid residues. However, in complex with NPC1L1, it showed conventional hydrogen bonding with GLU238, GLN88, and GLY65 while carbon-hydrogen bonding was shown with LEU81, and ASN132 amino acid residues. Moreover, hydrophobic interactions (alkyl, π-alkyl and π sigma) were shown with PRO131, CYS63, CYS109, THR83, and HIS126 amino acid residues (Fig. 5).

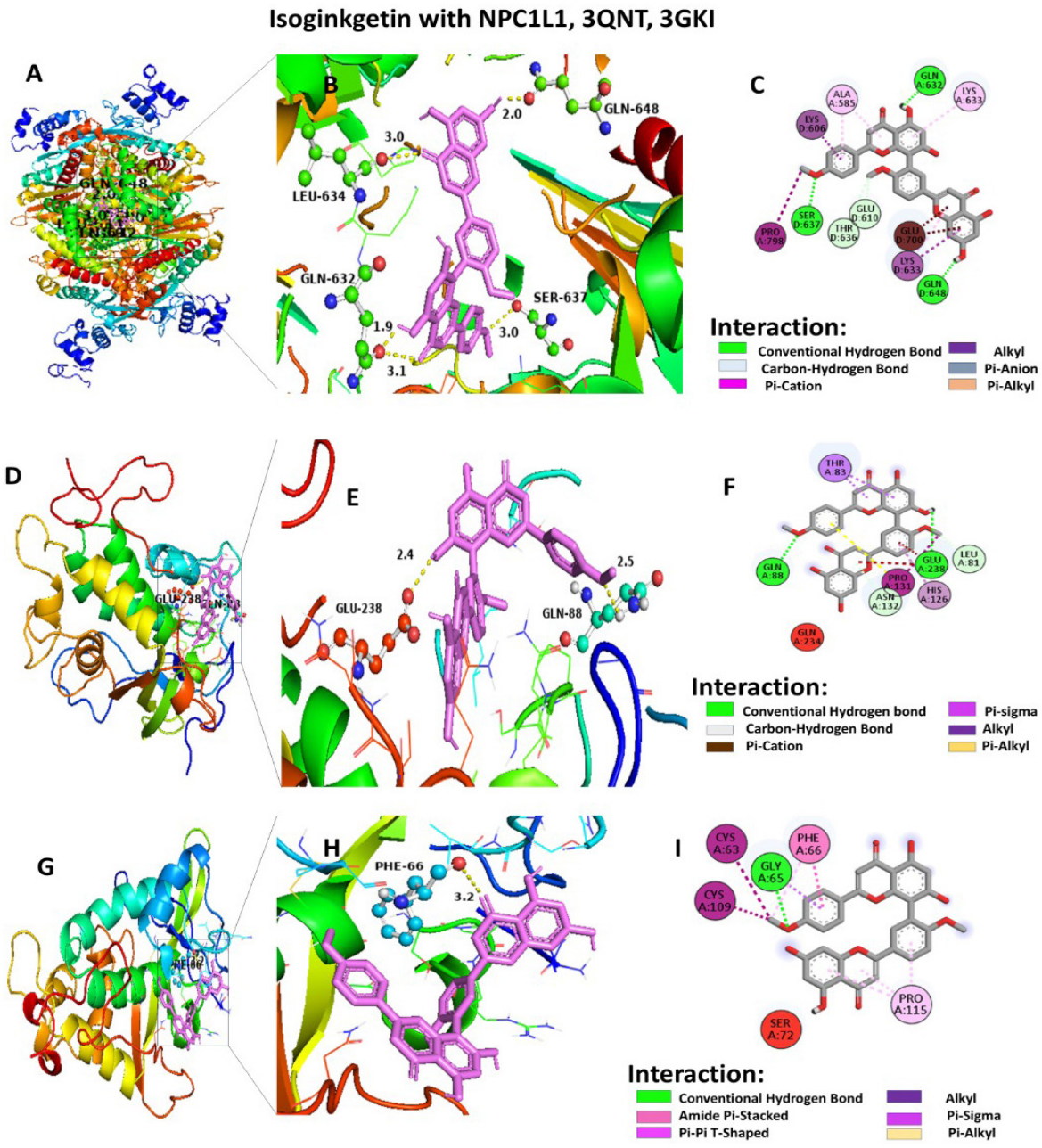


Fig. 5. Interactions between ligand isoginkgetin with two proteins named 1DQ8 and NPC1L1 (3QNT, and 3GKI), respectively. A, B and C show the NPC1L1- Isoginkgetin complex's interaction, while D, E and F show the 3QNT- Isoginkgetin complex's interaction, and G, H and I show the 3GKI- Isoginkgetin complex's interaction through PyMOL and Discovery Studio Visualizer.

Quercetin in complex with 1DQ8 showed conventional hydrogen bonding with GLU200, TRP698, SER637, and LYS606 amino acid residues, while hydrophobic interactions (π anion and π-alkyl) were shown with GLU610, PRO798, and ALA585 amino acid residues. While carbon hydrogen bonding shown with HIS635 amino acid residue. However, in complex with NPC1L1, it showed conventional hydrogen bonding with SER56, GLU38, SER102, GLN79, ARG39 and MET193 while π donor hydrogen bonding was shown with ASN41 amino acid residue. Moreover, hydrophobic interactions (π T shaped and π-alkyl) were shown with PHE108, GLN200, PRO215, LEU103, ALA201, and PRO202 amino acid residues (Fig. 6).

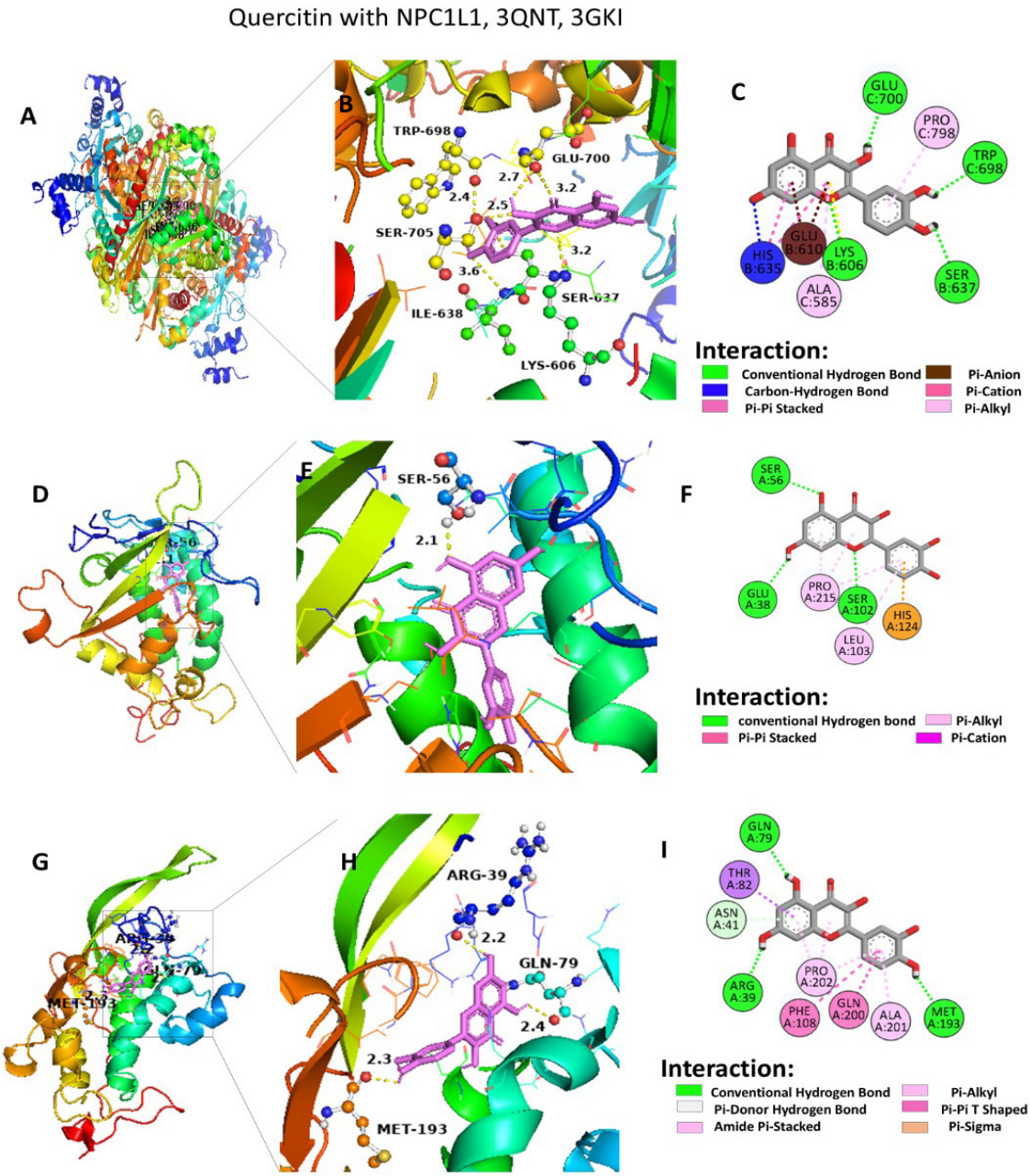


Fig. 6. Interactions between ligand quercitin with two proteins named 1DQ8 and NPC1L1 (3QNT, and 3GKI), respectively. A, B and C show the NPC1L1- Quercitin complex's interaction, while D, E and F show the 3QNT- Quercitin complex's interaction, and G, H and I show the 3GKI- Quercitin complex's interaction through PyMOL and Discovery Studio Visualizer.

Sakuranetin in complex with 1DQ8 showed conventional hydrogen bonding with SER637, and ILE638 amino acid residues, while hydrophobic interactions (π cation, π-stacked and π-alkyl) were shown with LYS606, PRO798, and GLU610 amino acid residues. Moreover, carbon hydrogen bonding shown with HIS635 amino acid residue. However, in complex with NPC1L1, it showed conventional hydrogen bonding with SER53, ASN86, and THR112 while carbon-hydrogen bonding was shown with SER102, and LEU213 amino acid residues. Moreover, hydrophobic interactions (alkyl and π-alkyl) were shown with ARG39, PRO202, PHE203, PHE108, LEU52, and ILE105 amino acid residues (Fig. 7).

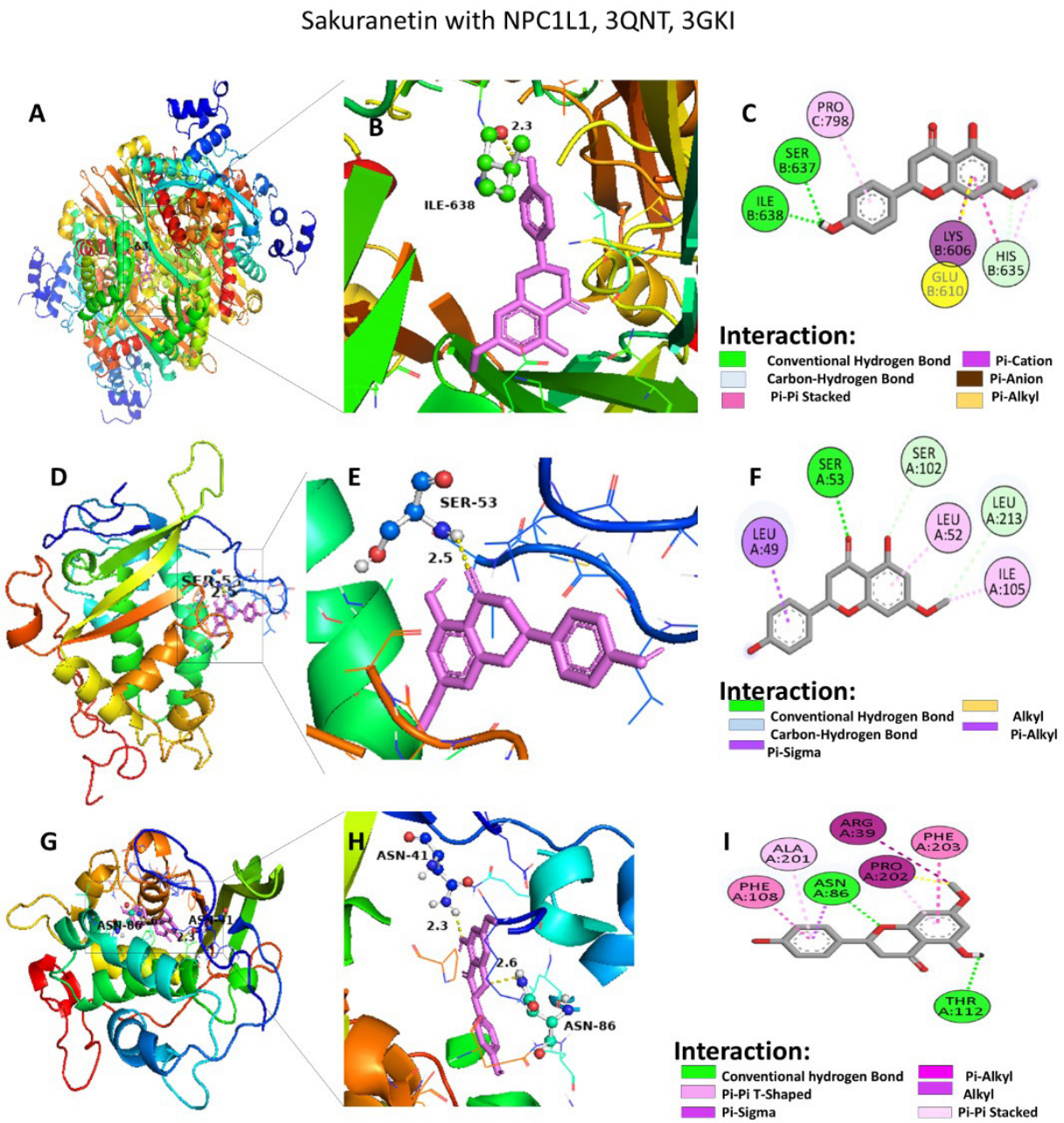


Fig. 7. Interactions between ligand sakuranetin with two proteins named 1DQ8 and NPC1L1 (3QNT, and 3GKI), respectively. A, B and C show the NPC1L1- Sakuranetin complex's interaction, while D, E and F show the 3QNT- Sakuranetin complex's interaction, and G, H and I show the 3GKI- Sakuranetin complex's interaction through PyMOL and Discovery Studio Visualizer.

DISCUSSION

Studied 25 bioactive phytochemicals of CPS fruit compounds to control hypercholesterolemia by using molecular docking and ADMET (absorption, distribution, metabolism, excretion, and toxicity) evaluation. Hypercholesterolemia is a major factor for cardiovascular disease (LaRosa, 2003). The studies bioactive compounds are involved in controlling the absorption and biosynthesis of cholesterol. The main principal molecular targets involved in these mechanisms include NPC1L1, which mediates intestinal cholesterol absorption, and HMG-CoA reductase, which controls the cholesterol biosynthesis. Clinically used drugs such as atorvastatin and ezetimibe act on these respective pathways (Chen *et al*., 2011; Schroor *et al*., 2021). However, long-term drug use may cause side effects, prompting the search for safer, plant-derived alternatives.

The lowest binding energies exhibited by NPC1L1 and HMG-CoA reductase highlights the anticholestrol potential of bioactive compounds from the fruit of CPS. The finding showed strong inhibitory potential and lower binding energies as compared to standard drugs. While flavonoids like Isoginkgentin, Quercetin, and ginkgetin showed lowest binding energies with both targets. Th flavonoids compound act as dual inhibitory mechanism as well as blocking intestinal cholesterol absorption (Zhang *et al*., 2022).

The physicochemical properties of the screened compounds further support their biological relevance. Corchoionoside C (MW 386.44 g/mol) has hydrogen bond donors (5), hydrogen bond acceptors (8), TPSA of 136.68 Å², and a WlogP of –0.58, suggesting moderate polarity and reasonable aqueous solubility. Daucosterol (MW 576.85 g/mol) and Ginkgetin (MW 566.51 g/mol) exhibit higher molecular weights and increased lipophilicity (WlogP 5.85 and 5.74, respectively), which may enhance membrane permeability but potentially reduce solubility. Glucosinolate (MW 478.49 g/mol) shows a high TPSA (224.81 Å²), indicating strong polarity and potential limitations in passive membrane diffusion. Isoginkgetin shares similar physicochemical parameters with Ginkgetin, while quercetin (MW 302.24 g/mol; WlogP 1.99; TPSA 131.36 Å²) displays balanced polarity and lipophilicity. Sakuranetin (MW 286.28 g/mol; TPSA 75.99 Å²; WlogP 2.49) exhibits comparatively lower polarity and favorable drug-like properties (Annaz *et al*., 2022) as given in Table III.

The ADMET profile of screened phytochemicals shows additional insights into their pharmacokinetic behavior. Corchoionoside C illustrates relatively high solubility (Log S –0.03) but low GI absorption and is forecasted to be a P-glycoprotein (P-gp) substrate, which may limit its bioavailability. Daucosterol and Ginkgetin show extremely low solubility (Log S –9.67 and –8.81, respectively) and low GI absorption, reflecting their high lipophilicity and molecular weight. Glucosinolate also presents low GI absorption and is predicted as a P-gp substrate, suggesting limited intestinal permeability (Zhang and Ma, 2018) as given in Table IV.

Table III. Lipinski's rule of five for selected CPS compounds.

Compound name	MW (g/mol)	H-Acceptor	H-Donor	TPSA Å²	Wlog P
Corchoionoside C	386.44	8	05	136.68	-0.58
Daucosterol	576.85	6	4	99.38	5.85
Ginkgetin	566.51	10	4	159.80	5.74
Glucosinolate	478.49	11	6	224.81	0.47
Isoginkgetin	566.51	10	4	159.80	5.74
Quercetin	302.24	7	5	131.36	1.99
Sakuranetin	286.28	5	2	75.99	2.49

Table IV. ADMET properties of the selected CPS compounds via SwissADME online tool.

Compounds	Corchoionoside C	Daucosterol	Ginkgetin	Glucosinolate	Isoginkgetin	Quercetin	Sakuranetin
Solubility Log *S* (ESOL)	-1.24	-7.70	-7.17	-2.42	-7.17	-3.16	-3.70
GI absorption	Low	Low	Low	Low	Low	High	High
BBB permeant	No	No	No	No	No	No	Yes
P-gp substrate	Yes	No	No	Yes	No	No	No
CYP1A2 inhibitor	No	No	No	No	No	Yes	Yes
CYP2C19 inhibitor	No	No	No	No	No	No	Yes
CYP2C9 inhibitor	No	No	Yes	No	Yes	No	No
CYP2D6 inhibitor	No	No	No	No	No	Yes	No
CYP3A4 inhibitor	No	No	No	No	No	Yes	Yes
Log K_p cm/s	-9.40	-4.32	-5.72	-9.30	-5.72	-7.05	-6.02

In contrast, quercetin and sakuranetin exhibit high GI absorption, showing better oral bioavailability. Sakuranetin is predicted to be BBB-permeant, while the other phytochemicals are not. The metabolic interaction profile indicates that quercetin may inhibit several cytochrome P450 enzymes, including CYP1A2, CYP2D6, and CYP3A4, which suggests possible drug–drug interactions but also highlights its metabolic activity. Sakuranetin is predicted to inhibit CYP1A2, CYP2C19, and CYP3A4, while ginkgetin and isoginkgetin iluctrate selective inhibition of CYP2C9. The skin permeability coefficient (Log Kp) values indicate generally low dermal absorption, with corchoionoside C and glucosinolate showing particularly low permeability (–9.40 and –9.30 cm/s, respectively).

The molecular docking results demonstrate that quercetin acts as a potential compound, exhibiting high docking scores with all targeted proteins (–9.4, –7.8, –8.6 kcal/mol). This shows its potential to inhibit cholesterol biosynthesis and absorption. The structure of quercetin, including multiple hydroxyl groups, enables strong hydrogen bonding and hydrophobic interactions within the active sites of both targets. Similarly, ginkgetin and isoginkgetin as biflavonoids, have extended aromatic systems and functional groups that enhance binding stability within the hydrophobic pockets of the target proteins (Šamec *et al*., 2022).

Daucosterol and β-carotene, representing sterol-like and carotenoid compounds, also demonstrate lipid-interacting capabilities. Phytosterols such as daucosterol structurally resemble cholesterol and may compete with it during intestinal absorption, thereby reducing serum cholesterol levels (Brauner *et al*., 2012). This mechanism complements the enzyme-inhibitory effects of flavonoids. The combined presence of flavonoids and phytosterols in CPS suggests a synergistic mode of action, targeting multiple steps in cholesterol metabolism.

On the other hand, smaller phytochemicals such as tetrahydropyran-2-one and uracil exhibited the binding energies of –4.7kcal/mol and –5.3 kcal/mol, respectively. Their limited interaction with the hydrophobic binding pockets of NPC1L1 and HMG-CoA reductase indicates poor structural compatibility and weaker inhibitory potential. This observation underscores the importance of molecular size, functional groups, and structural complexity in determining effective protein–ligand interactions.

Overall, the in silico findings support the anti-hypocholesterolemic potential of CPS phytochemicals, particularly flavonoids and phytosterols. The dual inhibition of NPC1L1 and HMG-CoA reductase represents a promising therapeutic strategy comparable to the combined effects of statins and cholesterol absorption inhibitors. Moreover, compounds such as quercetin and sakuranetin demonstrate favorable ADMET characteristics, especially in terms of gastrointestinal absorption, enhancing their candidacy as orally active agents.

However, despite the promising docking and pharmacokinetic predictions, it is essential to acknowledge the limitations of *in-silico* studies. The docking analysis employed a rigid-receptor approach, which does not account for protein flexibility or conformational changes that may occur upon ligand binding. In addition, molecular dynamics simulations were not performed to assess the stability of the predicted protein–ligand complexes over time. The docking assessment was also limited to the N-terminal domain of the target proteins, which may not fully represent the binding characteristics of the complete proteins. Furthermore, docking scores provide approximate estimates of binding affinity and may be influenced by scoring-function errors, ligand size, and molecular interactions that are not adequately captured by the scoring algorithm. Larger molecules may receive more favorable scores because of their greater number of potential interactions, potentially introducing size-related bias. The study also did not investigate selectivity or potential off-target interactions, limiting the ability to establish whether the predicted compounds specifically target HMG-CoA reductase and NPC1L1. Moreover, the pharmacokinetic and drug-likeness assessments relied on web-based prediction tools, which provide computational estimates rather than experimentally confirmed properties. Furthermore, *in vivo* studies are required to evaluate lipid-lowering efficacy, bioavailability, metabolic stability, and safety profiles.

CONCLUSION

The phytochemicals of CPS, particularly flavonoids such as Isoginkgetin, ginkgetin, and quercetin, along with phytosterols like daucosterol demonstrated significant potential against hypercholesterolemia. Their synergistic effects, multitargeted mechanisms, and favorable pharmacokinetic properties suggest that CPS fruit could serve as a promising natural source for the development of alternative lipid-lowering therapies. Future experimental validation will be crucial to translate these computational findings into clinically relevant applications.

DECLARATIONS

Acknowledgement

The authors would like to express their sincere gratitude to the Cancer Research Lab, Institute of Zoology,

University of the Punjab, Quaid-e-Azam Campus, Lahore, Pakistan, for providing the necessary facilities, computational resources, and research environment to conduct this study.

Funding

The study received no external funding.

Generative AI and AI assisted technology statement

No genarative AI or AI-assisted technology was used for this study.

Statement of conflict of interest

The authors have declared no conflict of interest.

REFERENCES

Annaz, H., Sane, Y., Bitchagno, G.T., Ben Bakrim, W., Drissi, B., Mahdi, I., El-Bouhssini, M. and Sobeh, M., 2022. Caper (*Capparis spinosa* L.): An updated review on its phytochemistry, nutritional value, traditional uses, and therapeutic potential. *Front. Pharmacol.*, **13**: 878749.

Axiotis, E., Halabalaki, M. and Skaltsounis, L.A., 2018. An ethnobotanical study of medicinal plants in the Greek islands of North Aegean region. *Front. Pharmacol.*, **9**: 409.

Bove, M., Cicero, A.F.G. and Borghi, C., 2019. Emerging drugs for the treatment of hypercholesterolemia. *Expert Opin. Emerg. Drugs*, **24**: 63–69.

Brauner, R., Johannes, C., Ploessl, F., Bracher, F. and Lorenz, R.L., 2012. Phytosterols reduce cholesterol absorption by inhibition of 27-hydroxycholesterol generation, liver X receptor α activation, and expression of the basolateral sterol exporter ATP-binding cassette A1 in Caco-2 enterocytes. *J. Nutr.*, **142**: 981–989.

Chen, J., Jiang, Y., Ma, K.Y., Chen, F. and Chen, Z.Y., 2011. Microalga decreases plasma cholesterol by down-regulation of intestinal NPC1L1, hepatic LDL receptor, and HMG-CoA reductase. *J. Agric. Fd. Chem.*, **59**: 6790–6797.

Coghlan, M.L., Maker, G., Crighton, E., Haile, J., Murray, D.C., White, N.E., Byard, R.W., Bellgard, M.I., Mullaney, I. and Trengove, R., 2015. Combined DNA, toxicological and heavy metal analyses provides an auditing toolkit to improve pharmacovigilance of traditional Chinese medicine (TCM). *Sci. Rep.*, **5**: 17475.

Fung, F.Y. and Linn, Y.C., 2015. Developing traditional Chinese medicine in the era of evidence-based medicine: Current evidences and challenges. *Evid. Based Complement. Altern. Med.*, **2015**: 425037.

Ge, L., Wang, J., Qi, W., Miao, H.H., Cao, J., Qu, Y.X., Li, B.L. and Song, B.L., 2008. The cholesterol absorption inhibitor ezetimibe acts by blocking the sterol-induced internalization of NPC1L1. *Cell Metab.*, **7**: 508-519.

Goldstein, J.L., 1974. *Familial hypercholesterolemia.*

Hassan, I., Zaman, A., Zafar, E. and Khan, M., 2024. Molecular docking-aided identification of natural bioactive molecules as potential cancer cell proliferation inhibitors: Molecular docking as cancer cell inhibitors. *Future Biotechnol.*, **4**: 25–30.

Jamshed, A., Bibi, A., Anwar, A., Qasim, A., Zafar, E. and Khan, M., 2025. *In silico* investigation of novel phytoactive compounds as ER-α inhibitors. *South Asian J. Zool.*, **1**: 29–35.

Khera, A.V. and Hegele, R.A., 2020. What is familial hypercholesterolemia, and why does it matter? *Circulation*, **141**: 1760–1763.

LaRosa, J.C., 2003. Understanding risk in hypercholesterolemia. *Clin. Cardiol.*, **26**(**S1**): 3–6.

Lee, H.H., Cho, S.M.J., Lee, H., Baek, J., Bae, J.H., Chung, W.J. and Kim, H.C., 2021. Korea heart disease fact sheet 2020: Analysis of nationwide data. *Korean Circ. J.*, **51**: 495–503.

Nordestgaard, B.G., Chapman, M.J., Humphries, S.E., Ginsberg, H.N., Masana, L., Descamps, O.S., Wiklund, O., Hegele, R.A., Raal, F.J. and Defesche, J.C., 2013. Familial hypercholesterolaemia is underdiagnosed and undertreated in the general population: Guidance for clinicians to prevent coronary heart disease. *Eur. Heart J.*, **34**: 3478–3490.

Rathee, S., Mogla, O., Sardana, S., Vats, M. and Rathee, P., 2010. Antidiabetic activity of *Capparis decidua* Forsk Edgew. *J. Pharma. Res.*, **3**: 231–234.

Šamec, D., Karalija, E., Dahija, S. and Hassan, S.T., 2022. Biflavonoids: Important contributions to the health benefits of Ginkgo (*Ginkgo biloba* L.). *Plants*, **11**: 1381.

Sarkar, B., Biswas, P., Adhikari, S., Roy, D., Kumar, B., Behera, N.R.M. and Erfani, H., 2025. *Pharmacological uses of new bioactive compounds from medicinal plants.*

Sayed, A., Navar, A.M., Slipczuk, L., Ballantyne, C.M., Samad, Z., Lavie, C.J. and Virani, S.S., 2023. Prevalence, awareness, and treatment of elevated LDL cholesterol in US adults, 1999–2020. *JAMA Cardiol.*, **8**: 1185–1187.

Schroor, M.M., Mokhtar, F.B., Plat, J. and Mensink, R.P., 2021. Associations between SNPs in intestinal cholesterol absorption and endogenous cholesterol

synthesis genes with cholesterol metabolism. *Biomedicines*, **9**: 1475.

Timmis, A., Vardas, P., Townsend, N., Torbica, A., Katus, H., De Smedt, D., Gale, C.P., Maggioni, A.P., Petersen, S.E. and Huculeci, R., 2022. European society of cardiology: Cardiovascular disease statistics 2021. *Eur. Heart J.*, **43**: 716–799.

von Känel-Cordoba, I., Wirnitzer, K., Weiss, K., Nikolaidis, P.T., Devrim-Lanpir, A., Hill, L., Rosemann, T. and Knechtle, B., 2024. Efficacy, side effects, adherence, affordability, and procurement of dietary supplements for treating hypercholesterolemia: A narrative review. *J. Hlth. Popul. Nutr.*, **43**: 189.

Wilemon, K.A., Patel, J., Aguilar-Salinas, C., Ahmed, C.D., Alkhnifsawi, M., Almahmeed, W., Alonso, R., Al-Rasadi, K., Badimon, L. and Bernal, L.M., 2020. Reducing the clinical and public health burden of familial hypercholesterolemia: A global call to action. *JAMA Cardiol.*, **5**: 217–229.

Xue, H., Huang, Y., Shah, A.M., Wang, X., Hu, Y., Zhang, L. and Zhao, Z.K., 2025. Improving cofactor promiscuity of HMG-CoA reductase from *Ruegeria pomeroyi* through rational design. *Biomolecules*, **15**: p.976.

Zeeshan, G., Naimat, W., Furqan, H. and Shuja, H., 2023. Prevalence, risk factors and implications of hypercholesterolemia in Pakistan. *IJS Glob. Hlth.*, **6**: e0319.

Zhang, H. and Ma, Z.F., 2018. Phytochemical and pharmacological properties of *Capparis spinosa* as a medicinal plant. *Nutrients*, **10**: 116.

Zhang, Y., Zhang, X., Xiao, Z., Zhang, X. and Sun, H., 2022. Hypoglycemic and hypolipidemic dual activities of extracts and flavonoids from *Desmodium caudatum* and an efficient synthesis of the most potent 8-prenylquercetin. *Fitoterapia*, **156**: 105083.